Simultaneous intercalation of lithium, potassium and strontium into graphite in molten salts medium

Inass El Hajj, Lucie Speyer, Sebastien Cahen, Pascal Berger, Ghouti Medjahdi, Philippe Lagrange, Claire Hérold

Simultaneous intercalation of lithium, potassium and strontium into graphite in molten salts medium

Inass El Hajj[a], Lucie Speyer[a], Sébastien Cahen[*a], Pascal Berger[b], Ghouti Medjahdi[a], Philippe Lagrange[a], Claire Hérold[a]

[a] Université de Lorraine, CNRS, IJL, F-54000 Nancy, France

[b] NIMBE, CEA, CNRS, Université Paris-Saclay, CEA Saclay, 91191, Gif sur Yvette Cedex, France

Abstract

The LiCl-KCl molten salts method has been used in order to intercalate strontium into graphite. Combination of X-Ray Diffraction (XRD) experiments and ion beam analyses attests the obtaining of a monophasic sample. Its chemical composition corresponds to the $Li_{0.2}K_{0.6}Sr_{0.4}C_6$ formula, revealing the synthesis of a quaternary Graphite Intercalation Compound (GIC), in agreement with the high repeat distance of 640 pm determined from its 00*l* XRD and with the 1D electronic density profile. The very high-quality data obtained by *hk*0 diffraction and rotating crystal method lead to a 2D organization of the intercalated sheet described by a large hexagonal unit cell containing 78 carbon atoms. Such quaternary phase including simultaneously alkali and alkaline-earth metals is unique and can only be prepared from molten salts method, opening new perspectives concerning graphite-based two-dimensional materials.

Keywords

Graphite intercalation compound, molten salts, 2D materials, alkaline-earth metal, XRD, nuclear microprobe.

1. Introduction

Since the discovery of superconductivity in the first stage CaC_6 GIC under a critical temperature of 11.5K [1], the scientific community has taken a drastic interest in Graphite Intercalation Compounds (GIC) to re-investigate this field of two-dimensional materials. Hence, many experiments have been carried out using various methods to synthesize new superconducting

Corresponding author: sebastien.cahen@univ-lorraine.fr
Institut Jean Lamour - UMR 7198 CNRS-Université de Lorraine
Campus ARTEM - 2 Allée André Guinier - B.P. 50840 54011 Nancy Cedex FRANCE

compounds beginning by metal vapor phase method. Then solid-liquid methods including liquid metallic alloys and even molten salts such as LiCl-KCl have been developed [2].

Alkali metals (A) are easily intercalated into graphite using vapor phase or solid-liquid method. On the contrary, the intercalation of alkaline-earth (AE) and lanthanides (Ln) metals by solid-vapor method requires a reaction at high temperature which could lead to the destruction of the graphite network and the simultaneous formation of metal carbides. At moderate temperature, only an incomplete intercalation occurs due to a too low vapor pressure of the metal. Regarding these results, solid-liquid intercalation reactions in alkali-based molten alloys have been performed. Unfortunately, such a solid-liquid process also presents some limitations as several AE and Ln metals cannot be intercalated into graphite. In order to circumvent this pitfall, the use of an eutectic medium in which the metal to intercalate is soluble allows to carry out reactions at low temperature and with a high chemical activity of the metal in this liquid medium. Thus, in 1992, A. Hérold *et al.* demonstrated that graphite remains intact towards pure liquid LiCl-KCl mixture and that its immersion in this eutectic after the dissolution of metallic lithium leads to the synthesis of the first stage LiC_6 compound [3]. Indeed, the eutectic mixture LiCl-KCl has shown its ability to dissolve a certain amount of A, AE and Ln metals at moderate temperature by displacement reaction with lithium [4]. The latter consists in the dissolution of a metal M accompanied with the following redox reaction: $n\ Li^+ + M \rightarrow n\ Li + M^{n+}$.

A more advanced study of the intercalation of metals into graphite in LiCl-KCl medium was then published in 1996 by Hagiwara *et al*. [5]. Their work, involving the use of lanthanide trichlorides, resulted in the formation of various LnC_6 intercalation compounds, in mixture with K_3LnCl_6 chlorides.

Inspired by these previous works, the study of the intercalation of alkali metals, alkaline earth metals and lanthanides in eutectic medium was pursued by our team [6]. In particular, the reactivity of graphite towards lanthanides was evaluated, in the absence of any trichlorides. The use of pyrolytic graphite platelet as host material allows an easy extraction and recovery of the sample from the molten chlorides medium. The synthesized sample is obtained in the form of a platelet, which makes possible in-depth structural studies.

Thus, this synthesis method had shown remarkable results allowing the intercalation of metals into graphite, as firstly verified by the synthesis of bulk binary EuC_6 compound [7]. Thereafter, several fully intercalated compounds have been synthesized including, either binary ones like

SrC_6 [8], BaC_6 [9] or even novel quaternary compounds such as $Li_{0.2}K_{0.75}Ba_{0.6}C_6$ [10]. This last one has given the opportunity to explore the co-intercalation of different alkali metals in the van der Waals gaps.

Here, we present the discovery of a novel strontium-based GIC prepared by the co-intercalation of lithium, potassium and strontium. This compound has undergone a full structural study revealing analogies and differences with other quaternary GIC recently synthesized in the Ba/LiCl-KCl system [11].

2. Experimental

2.1. Synthesis

The experiments are carried out in a glove box under argon atmosphere to avoid the reactivity towards air and moisture of the used reactants and reaction products. The novel Sr-based GIC is synthesized by adding 2 at.% of strontium in a LiCl-KCl eutectic medium as described in previous works [8-10].

At this step, a redox reaction occurs between lithium ions and metallic strontium following:

$$2Li^+ + Sr \rightarrow 2\ Li + Sr^{2+} \quad (1)$$

In a second step, native metallic lithium reacts with graphite leading to the formation of the corresponding first stage GIC:

$$Li + 6\ C \rightarrow LiC_6 \quad (2)$$

Finally, some substitution of the intercalated species can be observed, leading to binary or novel poly-layered intercalation compound, depending on the reaction conditions.

For this synthesis, a PGCCL (PyroGraphite Comprimé Carbone Lorraine) graphite platelet attached to a tungsten sample holder is immersed in this liquid in a stainless-steel reactor. The stirring, for little amount of time, of this heated molten mixture has already been shown to enhance the formation of compounds containing poly-layered intercalated sheets [10, 11]. The intercalation reaction is performed outside the glove box for 8 days at 450°C in a furnace with oscillations to enhance the homogeneity of the reactive medium. The preliminary experiments show the importance of these two steps of homogenization, hence the dissolution of enough amount of strontium to initiate the formation of this kind of compounds. Ultimately, the final step is performed inside the glove box. Therefore, the sample is removed from the molten mixture, manually scrapped and then positioned in a suited sample-holder sealed under argon for further characterization.

2.2. X-ray diffraction experiments

A full structural study is conducted using various X-ray diffraction experiments. The measurements are mostly performed with a Bruker D8 Advance diffractometer ($\lambda_{MoK\alpha1}$ = 70.926 pm) using (θ, 2θ) configuration mode and boosted with a solar slit (2.5°). As previously described, this GIC is prepared from a pyrolytic graphite platelet allowing to record 00*l* and *hk*0 reflections separately. Pyrolytic graphite platelets can be described as a single crystal along the c-axis but as crystallites are randomly distributed in the ab-plane, it is considered as a powder in this orientation.

The 00*l* reflections diagram allows the determination of the interplanar distance d_i and the stage. The quantitative analysis of these 00*l* reflections permits the determination of the electronic density profile along the *c*-axis and the stacking sequence of the atomic planes [12]. Then, the *hk*0 diagram helps to determine the two-dimensional unit cell according to the commensurability model developed by Lagrange *et al.* [13]. For indexation and intensity determination on 00*l* diffraction pattern, Bruker Diffrac.EVA software has been used.

Finally, a rotating crystal diffraction pattern is realized using a Bruker Kappa APEX diffractometer equipped with a two-dimensional CCD APEX II detector and an X-ray microsource (diameter spot 250 mm; $\lambda_{MoK\alpha1}$ = 70.936 pm). A small sample positioned in a Lindemann capillary (diameter = 0.5 mm) is used in these experiments.

2.3. Ion beam analysis

The experimental conditions involved in this study are a $^{1}H^{+}$ proton ion beam of 3000 keV of lateral size 3 x 3 µm² in scanning mode on 200 x 200 µm² windows. The SimNRA software has been used in order to interpret the collected data in simulations [14]. The cross sections used for nuclear reactions and backscattering are listed below. Except for strontium, most of backscattering cross-sections are non-Rutherford:

- Nuclear reaction on ^{7}Li ^{7}Li (p, α)^{4}He (laboratory data). Surface α particles are emitted at 7450 keV;
- Backscattering on lithium ^{7}Li [15]; ^{7}Li(p, p). Surface backscattered protons are emitted at 1680 keV;
- Backscattering on lithium ^{6}Li [15]; ^{6}Li(p, p)^{6}Li. Surface backscattered protons are emitted at 1530 keV;
- Backscattering on carbon ^{12}C(p, p)^{12}C[16]. Surface backscattered protons are emitted at 2145 keV;

- Non-Rutherford backscattering on oxygen $^{16}O(p, p)^{16}O$, [17]. Surface backscattered protons are emitted at 2320 keV;
- Backscattering on chlorine $^{nat}Cl(p, p)^{nat}Cl$, [18]. Surface backscattered protons are emitted at 2670 keV;
- Backscattering on potassium $^{nat}K(p, p)^{nat}K$, [19]. Surface backscattered protons are emitted at 2700 keV;
- Rutherford backscattering on $^{86\text{-}88}Sr$ isotopes (mainly $^{88}Sr(p, p)^{88}Sr$). Surface protons are emitted at 2870 keV.

3. Results and discussion

After synthesis, the recovered sample consists in a dilated light blue platelet, first evidences that an intercalation reaction occurred. The 00*l* X-ray diffraction pattern (Figure 1) reveals a main set of seven reflections that indicates the presence of a single phase intercalated into the bulk sample. Elsewhere, very small Bragg peaks imply the presence of a small amount of residual graphite and LiCl-KCl salts on the surface of the sample. From this diagram, the main peaks are easily indexed and lead to a first stage compound with a repeat distance of 640 pm ± 1 pm. The intensity of the 002 reflection is very strong, the second more intense which is the 004 reaches only 15% of the 002 one and the other peaks remain quite weak.

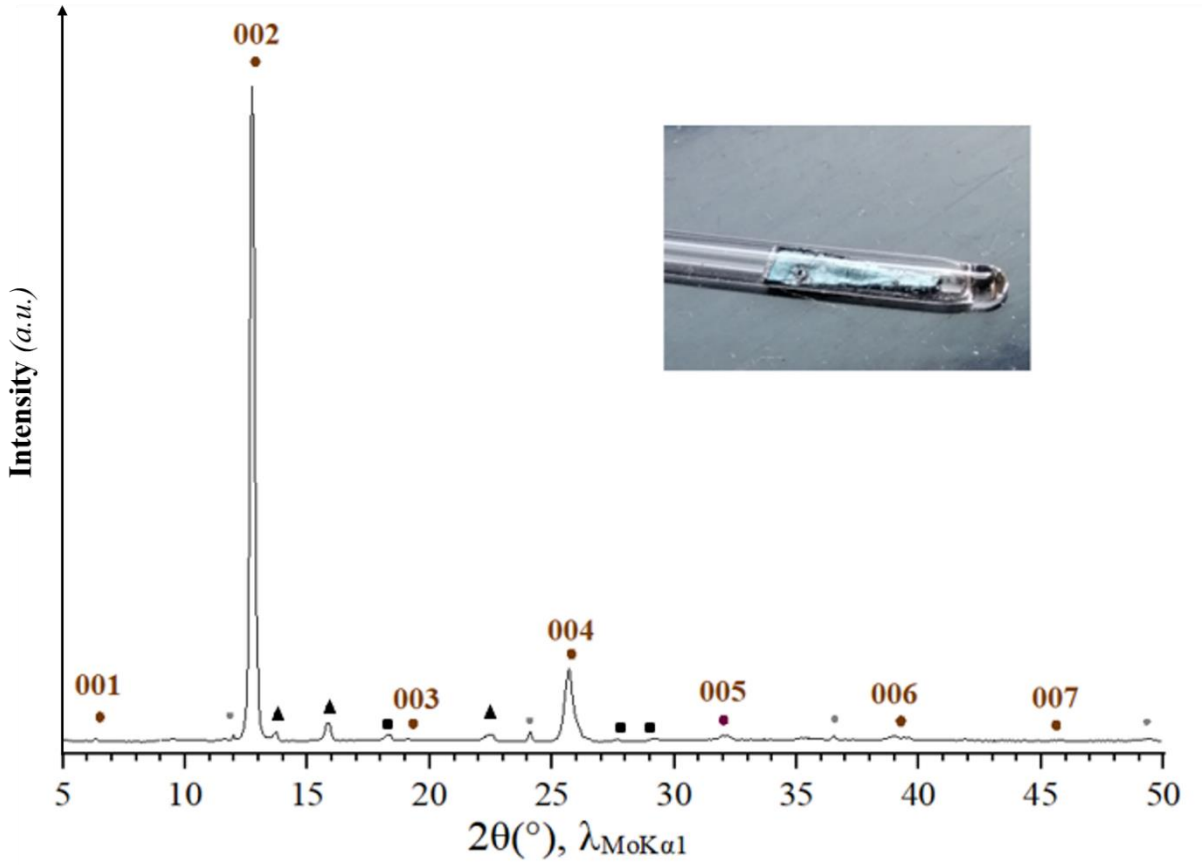

Figure 1: 00*l* X-ray diffractogram of the Sr-based GIC and picture of the corresponding sample (● $ICDD_{graphite}$: 04-007-2081 – ■ $ICDD_{LiCl}$: 04-016-2980 – ▲$ICDD_{KCl}$: 04-007-3113)

In order to confirm the exclusive presence of a single GIC in the sample, complementary analyses must be performed to prove the absence of any nanometric or amorphous phase. Ion beam analysis can be used to probe the chemical composition of the GIC, laterally and in-depth [20] and gives complementary information to those retrieved from XRD analyses. Different areas of several samples have been measured, and a representative spectrum is given in **Figure 2**.

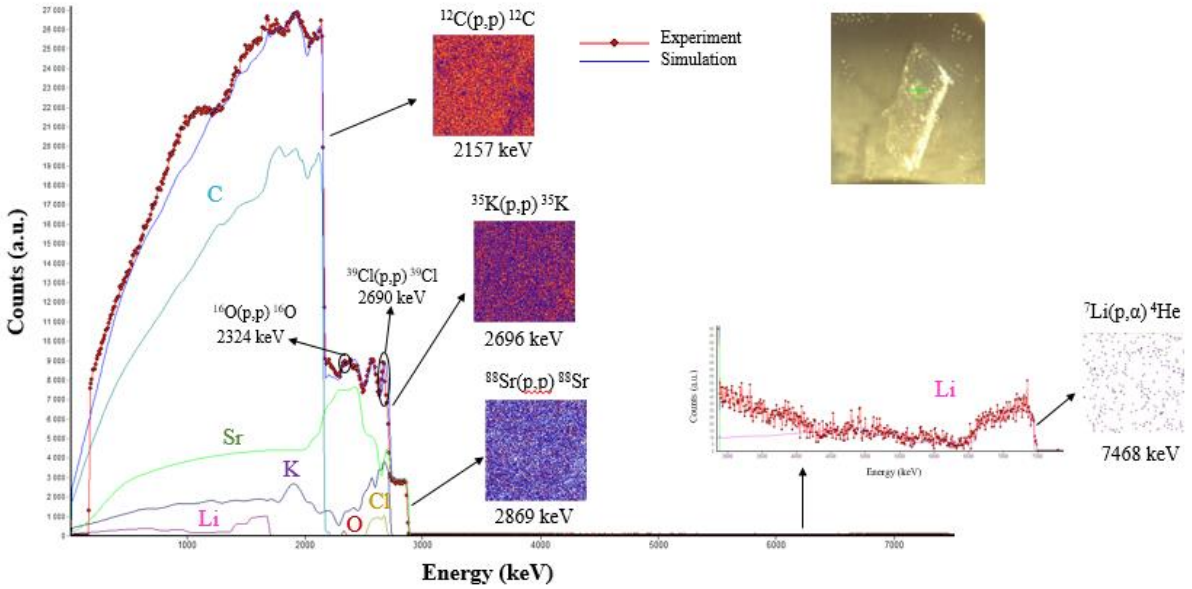

Figure 2: recorded RBS/NRA spectrum of the K-Li-Sr GIC and its simulation. Each individual elementary contribution to the simulation is drawn. Red spots: experiment; blue solid line: simulation. Inset shows a sample picture on the sample-holder of the microprobe instrument.

First, the remarkable homogeneity of the sample should be pointed out. Indeed, the maps corresponding to the different regions of interest selected in the spectrum for lithium, strontium, potassium and carbon all show that these elements are uniformly distributed. Considering the 00*l* X-ray data that can be indexed as a first stage GIC, and regarding that the ion beam analysis does not exhibit any heterogeneity laterally or in-depth, this analysis agrees with the composition of a single phase, not a mixture of several GIC.

A little contamination of the sample with chlorine and oxygen is detected, but these elements only lay on the surface of the sample as they are revealed by peaks instead of steps on the spectrum. Their presence is respectively due to the method of synthesis and to the air exposure during the transfer of the sample into the nuclear microprobe device. The simulation of the data also reveals a little migration of lithium at the surface of the sample, once again probably due to the air exposure. This is highlighted by the peak representing a surface over-concentration in lithium at very high energy (7000-7500keV).

Except these heterogeneities, the spectrum is well fitted considering a global $Li_{0.2}K_{0.6}Sr_{0.4}C_6$ formula for the bulk target.

The quantitative study of the 00*l* reflections allows to calculate the structure factor of each reflection in order to determine the *c*-axis electronic density profile of the compound. The 00*l*

structure factors (F_{00l}) calculated from a model are compared with those deduced from the experimental diffracted intensities. Both corresponding *c*-axis electronic density profiles obtained by Fourier transform of the F_{00l} are compared and superimposed [12]. The best agreement between experimental and calculated data is obtained with a three-layered intercalated sheet between graphene planes made of a central plane of strontium surrounded by two layers of mixed lithium and potassium atoms. The model is also based on the chemical composition obtained by ion beam analysis. The residual factor reaches 9%, considering a global thermal displacement (B = 1.9 $Å^2$), which confirms the good agreement between model and experiment.

The details of the experimental and calculated structure factors of the 00*l* reflections are given in Table 1. The comparison between corresponding *c*-axis electronic density profiles, and the detailed stacking sequence describing the model are respectively represented Figures 3 and 4.

Table 1: experimental and calculated structure factors of the 00*l* reflections of the first stage $Li_{0.2}K_{0.6}Sr_{0.4}C_6$

00*l*	**2θ** *(°, $\lambda_{MoK\alpha 1}$)*	**d_{00l}** *(pm)*	**F_{00l} exp.**	**I_{00l} exp.**	**F_{00l} calc.**	**I_{00l} calc.**
001	6.34	641.9	-20.4	8.3	-20.4	8.3
002	12.55	319.7	100.0	100.0	100.0	100.0
003	18.85	213.0	-5.9	0.2	-12.8	1.1
004	25.30	159.7	56.3	15.1	52.8	13.3
005	31.75	128.4	-18.8	1.3	-14.8	0.8
006	38.35	106.4	25.4	1.9	32.5	3.1
007	45.03	91.2	-15.4	0.6	-15.6	0.6

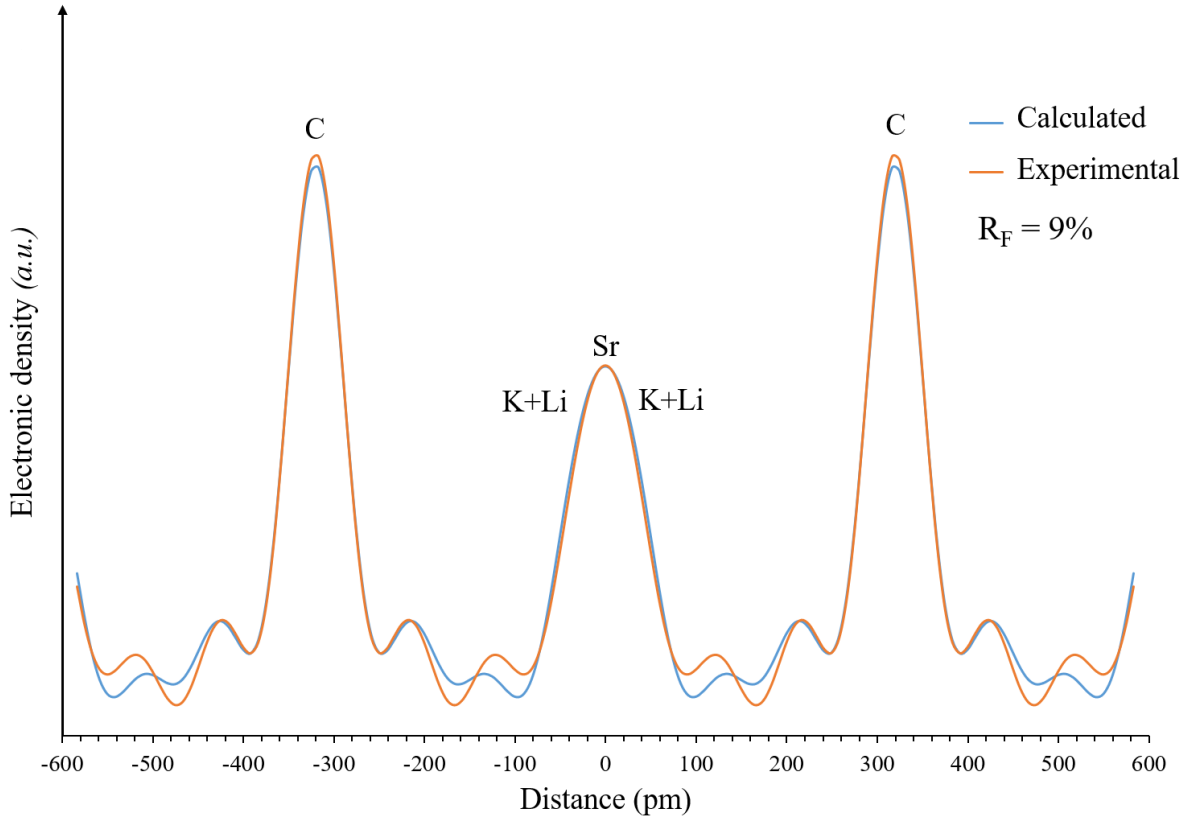

Figure 3: *c*-axis electronic density profile of the first stage $Li_{0.2}K_{0.6}Sr_{0.4}C_6$.

This quantitative modelling of the 00*l* XRD pattern agrees with the presence of a single phase in the sample. It should be noted that even lithium, a light element not easily detected by XRD, appears as an element belonging to the intercalated sheet. Indeed, the modelling is improved when lithium is taken into account among the intercalated atomic planes.

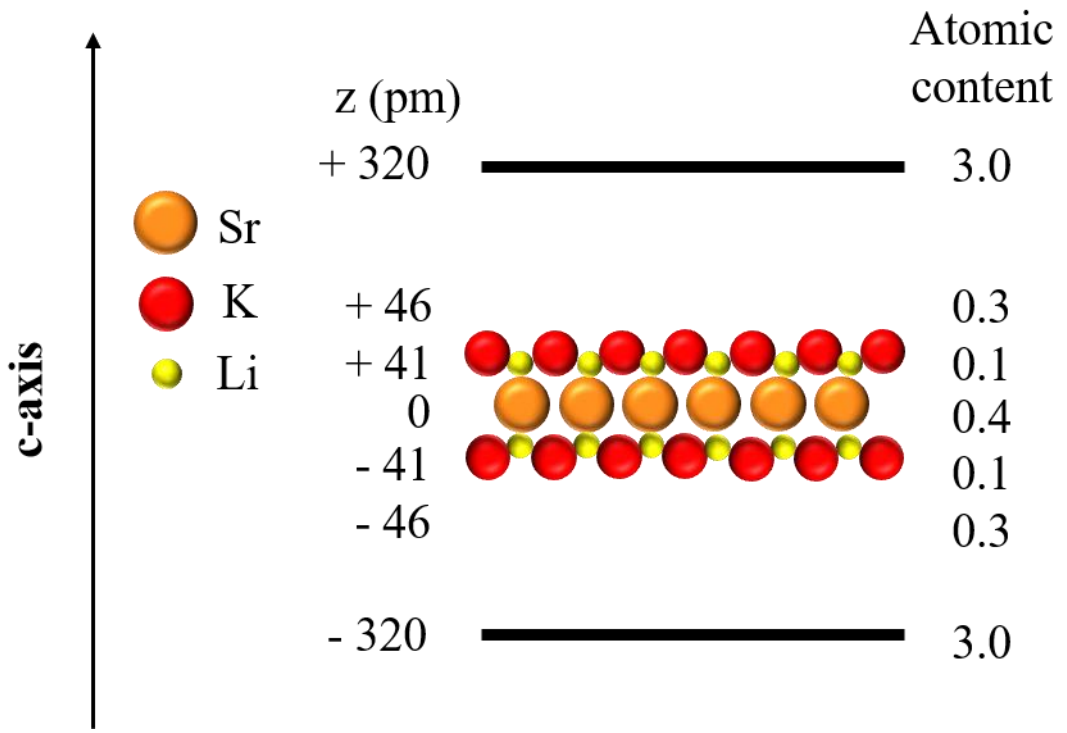

Figure 4: *c*-axis schematic stacking sequence of the first stage $Li_{0.2}K_{0.6}Sr_{0.4}C_6$.

The *hk*0 and *hkl* reflections were recorded in order to determine the unit cell parameters. The *hk*0 X-ray diffraction pattern (Figure 5) exhibits, in addition to the reflections due to the deposition of thin layer of chlorides on sample surface, the family of *hk*0 peaks of the Li-K-Sr GIC. Some of them correspond to the reflections of pristine graphite, revealing that the 2D in-plane lattice of the intercalated sheets is commensurate with respect to the graphenic one. Indeed, the reflections detected at 2θ equal to 19.15, 33.3 and 38.7° for the Li-K-Sr GIC are located at the same theoretical angular positions as the 100, 110 and 200 reflections of graphite. Thanks to the mathematical approach proposed by Lagrange *et al.* [13], an exhaustive inventory of all commensurate two-dimensional lattices was done for a given number of carbon atoms. Only one 2D lattice allowed a full indexation of all *hk*0 reflections, as presented Figure 5. It consists in a hexagonal 2D unit cell containing 78 carbon atoms, with $a = a_g \sqrt{39} = 1536$ pm ± 1 pm and rotated by 43° with respect to that of the graphene sheets, leading to the expression $(\sqrt{39} \times \sqrt{39})$R43° (Figure 6).

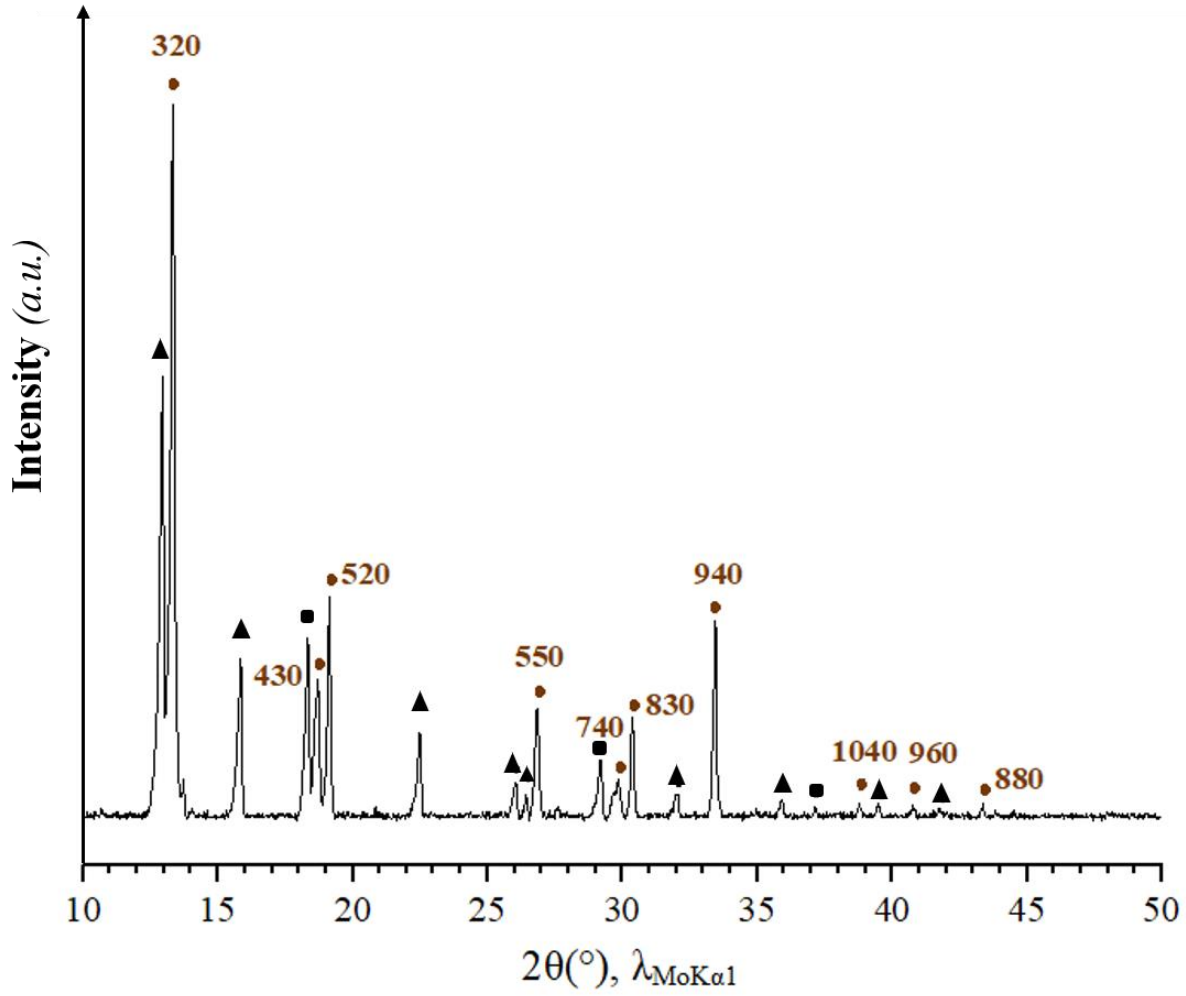

Figure 5: *hk*0 XRD pattern of the first stage $Li_{0.2}K_{0.6}Sr_{0.4}C_6$ (●) with detection of residual chlorides (■ $ICDD_{LiCl}$: 04-016-2980 – ▲ $ICDD_{KCl}$: 04-007-3113).

To complete the structural study of this GIC, a rotating crystal pattern (Figure 7) was recorded on a small sample in order to investigate its 3D structure. Indeed, even if the sample is not a single crystal, this experiment allows to collect information about the three-dimensional structure such as the stacking sequence of graphene layers and intercalated sheets.

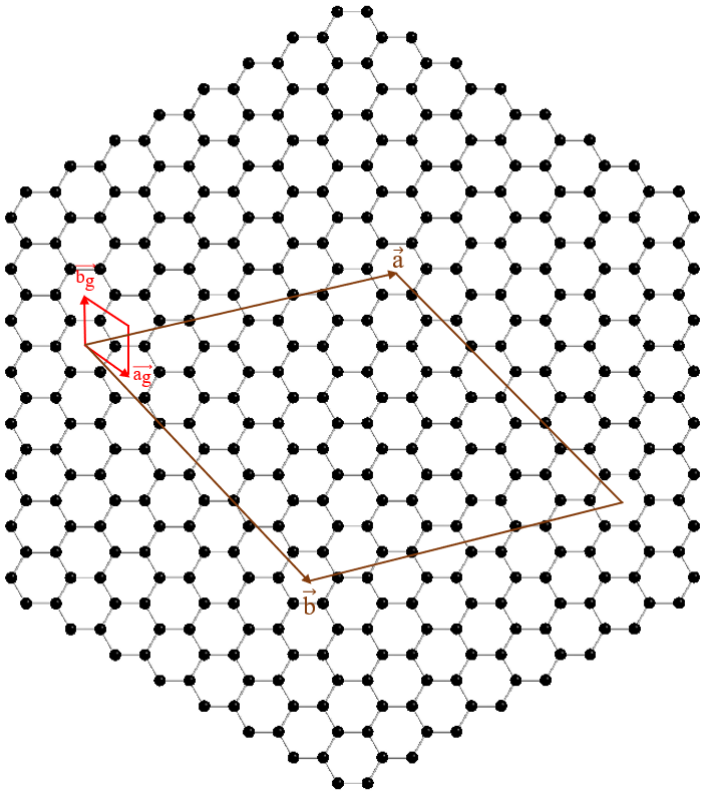

Figure 6: 2D lattices of graphite (—) and of the first stage $Li_{0.2}K_{0.6}Sr_{0.4}C_6$ (—) rotated by 43° from each other.

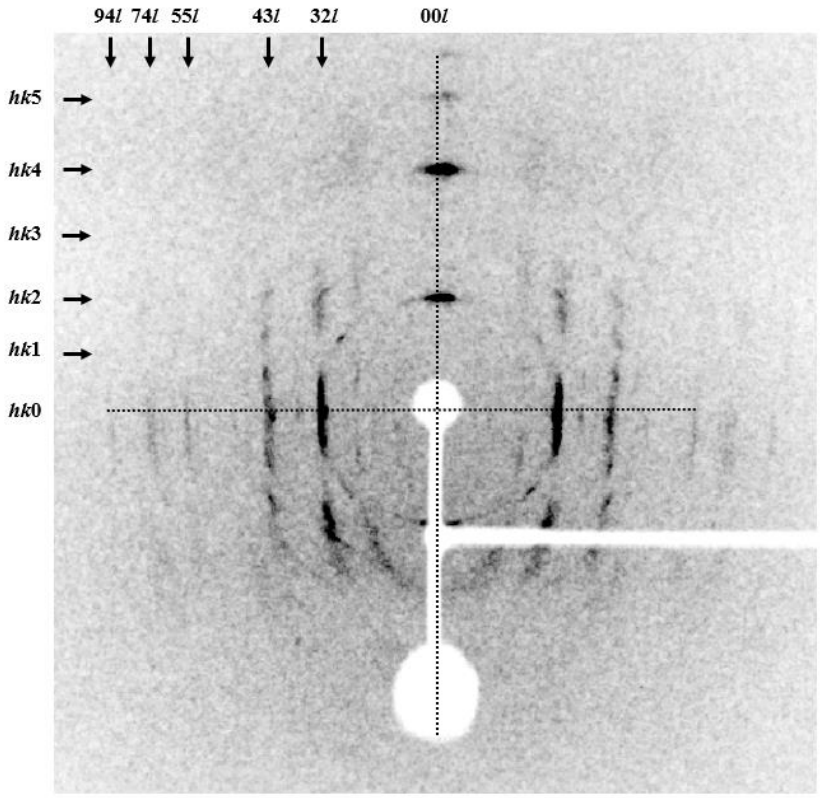

Figure 7: rotating crystal pattern of the first stage $Li_{0.2}K_{0.6}Sr_{0.4}C_6$.

All the strata were easily identified and indexed. The 320 reflection of the equatorial stratum is the most intense, which is in good agreement with the recorded *hk*0 diffractogram and the position of the *hk*0 stratum is used to confirm the value of the basal a parameter (1536 pm). Moreover, as in the 00*l* diffractogram, the 002 and 004 reflections are the most intense. The determination of the c parameter is possible from the *hkl* strata: indeed, the *hk*1 stratum is aligned with the calculated position of the 001 reflection indicating that the c parameter is equivalent to the repeat distance, *i.e.* 640 pm so that the stacking sequence of this compound is then AαAα...(A represents the graphene sheet and α the intercalated sheet).

To summarize the structural study of $Li_{0.2}K_{0.6}Sr_{0.4}C_6$, this GIC crystallizes in a hexagonal unit cell, commensurate with that of graphite $(\sqrt{39} \times \sqrt{39})R43°$ with the following parameters: a = 1536 pm ± 1 pm and c = 640 pm ± 1 pm.

On one hand, these structural data can be compared with those of SrC_6 [8]. On the other hand, analogies can be observed with a similar compound prepared in the Ba/LiCl-KCl system [11]. First, $Li_{0.2}K_{0.6}Sr_{0.4}C_6$ and SrC_6 can be compared regarding their stacking sequences (Figure 8).

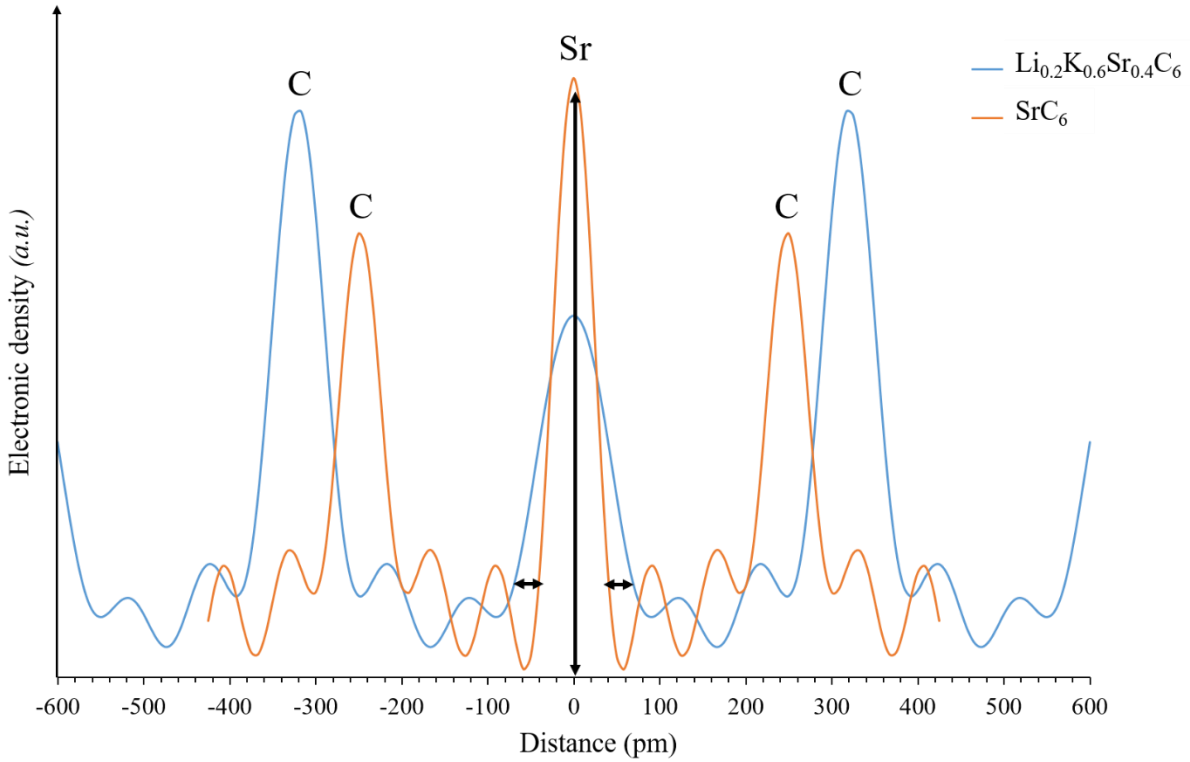

Figure 8: *c*-axis electronic density profiles of $Li_{0.2}K_{0.6}Sr_{0.4}C_6$ and SrC_6

The electronic density on the central layer is wider in the case of $Li_{0.2}K_{0.6}Sr_{0.4}C_6$ than SrC_6, due to the presence of adjacent lithium and potassium layers. Even if the quaternary compound contains a higher amount of metals (general formula $M_{1.2}C_6$), the overall electronic density is weaker than for SrC_6.

As mentioned earlier, a similar GIC has been evidenced from the reaction of graphite with barium dissolved in the same reaction medium [11]. It appears that these GIC have equivalent chemical compositions ($Li_{0.2}K_{0.6}Sr_{0.4}C_6$ and $Li_{0.2}K_{0.6}Ba_{0.35}C_6$) and exhibit the same light blue color. Moreover, they present similar repeat distances (640 pm ± 1 pm for the Sr-based GIC versus 650 ± 1 pm for the Ba-based one). The stacking sequences of these two GIC are shown Figure 9.

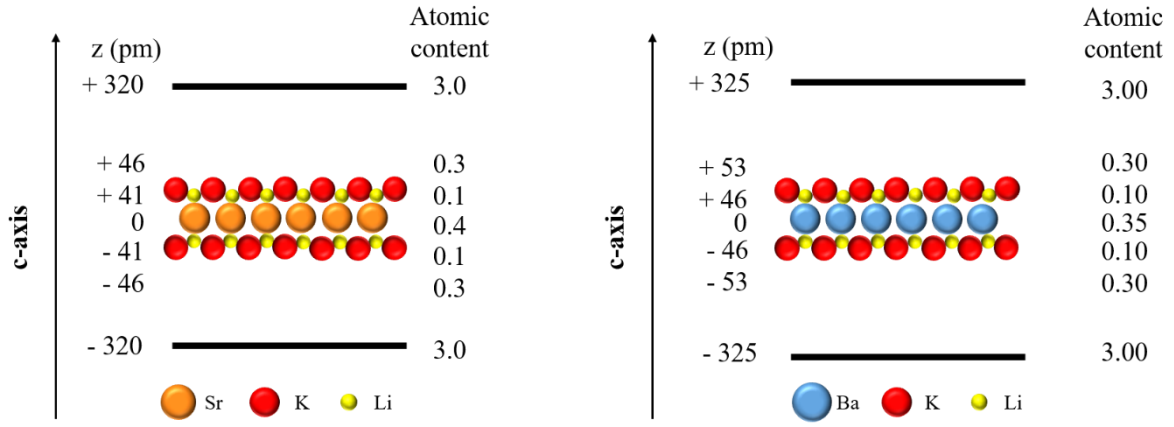

Figure 9: comparison of the schematic *c*-axis stacking sequences of $Li_{0.2}K_{0.6}Sr_{0.4}C_6$ and $Li_{0.2}K_{0.6}Ba_{0.35}C_6$

The higher ionic radius for Ba^{2+} than for Sr^{2+} explains the slightly higher value of the repeat distance for the barium-based compound, despite the similar chemical compositions. For both compounds, two layers of lithium and potassium surround the central alkaline-earth metal layer. The positions of the different atomic planes along *c*-axis are also comparable. For the strontium-based compound, the distance between the graphene layers and the mean position of the (K+Li) layers is equal to 276.5 pm, slightly higher than this same distance for the barium-based compound (273 pm). It is worth noting that they remain higher than the distance between potassium and graphene layers in the well-known first stage binary KC_8 compound (267.5 pm). The 2D lattices of SrC_6, $Li_{0.2}K_{0.6}Sr_{0.4}C_6$ and $Li_{0.2}K_{0.6}Ba_{0.35}C_6$ are compared Figure 10.

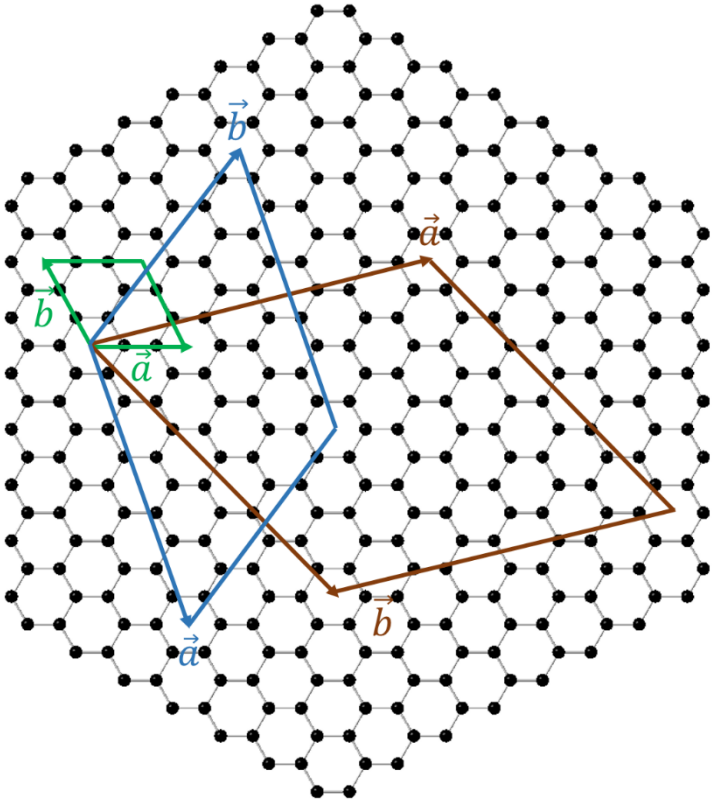

Figure 10: 2D lattices of SrC_6 (green), $Li_{0.2}K_{0.6}Sr_{0.4}C_6$ (brown) and $Li_{0.2}K_{0.6}Ba_{0.35}C_6$ (blue)

The 2D lattice of $Li_{0.2}K_{0.6}Sr_{0.4}C_6$ is much larger than that of SrC_6: the same difference is observed between BaC_6 and $Li_{0.2}K_{0.6}Ba_{0.35}C_6$. It is interesting to note that for the compounds containing poly-layered intercalated sheets, even if they present great similarities regarding their structure along *c*-axis (repeat distance and stacking sequence), their 2D lattices are quite different, both through their size and orientation. Such different planar cells between GIC with analogue composition have already been pointed out for graphite intercalated with bismuth or antimony and alkali metals [21, 22].

4. Conclusion

Intercalation of alkaline-earth metals into graphite remains challenging due to poor affinity of these metals for graphite. In the last years, we developed a novel way of synthesis using LiCl-KCl eutectic molten mixture in order to dissolve alkaline-earth metals. It has subsequently been possible to intercalate barium and strontium, leading to corresponding MC_6 binary compounds. Very recently, we showed the possibility to prepare a quaternary barium-based GIC by modifying several experimental parameters. By transferring the method to the

LiCl-KCl/Sr system, we succeeded in the preparation of a novel quaternary GIC, analogous in composition and repeat distance with the one prepared in the LiCl-KCl/Ba system. It consists in a $Li_{0.2}K_{0.6}Sr_{0.4}C_6$ compound with a repeat distance equals to 640 pm, a bit smaller than the one of the barium-based phase (650 pm) mainly due to a smaller ionic radius. This repeat distance is also in agreement with a (K,Li)-Sr-(Li,K) three-layered intercalated sheet determined by the 1D electronic density profile of the compound. As 00*l* XRD pattern reveals only one family of Bragg peaks that can be modeled considering the aforementioned stacking sequence and regarding the homogeneity of the elementary maps retrieved from ion beam analysis, we attest the obtaining of a single-phase sample.

It has also been possible to determine its two-dimensional unit cell by the combination of various X-ray diffraction techniques and a commensurability model developed in our team. The $Li_{0.2}K_{0.6}Sr_{0.4}C_6$ compound exhibits a very large $(\sqrt{39} \times \sqrt{39})R43°$ 2D hexagonal unit cell, and we conclude on the following lattice parameters for this quaternary GIC: a = 1536 pm ± 1 pm and c = 640 pm ± 1 pm.

Statment and declarations

Competing interest

The authors declare that they have no known competing financial interests or personal relationships that could have appeared to influence the work reported in this paper.

Conflict of interest

On behalf of all authors, the corresponding author states that there is no conflict of interest.

References

[1] N. Emery, C. Hérold, M. d'Astuto, V. Garcia, Ch. Bellin, J. F. Marêché, P. Lagrange, G. Loupias, Superconductivity of bulk CaC_6. Phys. Rev. Lett. 95 (2005) 087003. https://doi.org/10.1103/PhysRevLett.95.087003

[2] S. Cahen, L. Speyer, P. Lagrange, C. Hérold, Topotactic Mechanisms Related to the Graphene Planes: Chemical Intercalation into Graphite of Electron Donors, Eur. J. Inorg. Chem. 2019 (2019) 4798-4806. https://doi.org/10.1002/ejic.201900758

[3] A. Hérold, M. Lelaurain, J. F. Marêché. Intercalation of ionic compounds into graphite, Proceedings International Carbon Conference. (1992) 571-573.

[4] A. J. Bard, J. A. Plambeck, Encyclopedia of electrochemistry of the elements - X Fused salt systems, Marcel Dekker, New York (1976).

[5] R. Hagiwara, M. Ito, Y. Ito, Graphite intercalation compounds of lanthanide metals prepared in molten chlorides, Carbon. 34 (1996), 1591-1593. https://doi.org/10.1016/S0008-6223(96)00109-1

[6] S. Cahen, I. El Hajj, L. Speyer, P. Berger, G. Medjahdi, P. Lagrange, G. Lamura, C. Hérold, Original synthesis route of bulk binary superconducting graphite intercalation compounds with strontium, barium and ytterbium, New J. Chem. 44 (2020) 10050-10055. https://doi.org/10.1039/C9NJ06423K

[7] M. Bolmont, S. Cahen, M. Fauchard, R. Guillot, G. Medjahdi, P. Berger, G. Lamura, P. Lagrange, C. Hérold, LiCl-KCl eutectic molten salt as an original and efficient medium to intercalate metals into graphite: Case of europium, Carbon. 133 (2018) 379-383. https://doi.org/10.1016/j.carbon.2018.03.015

[8] I. El Hajj, L. Speyer, S. Cahen, P. Lagrange, G. Medjahdi, C. Hérold, Crystal structure of first stage strontium-graphite intercalation compound, Carbon. 168 (2020) 732-736. https://doi.org/10.1016/j.carbon.2020.05.102

[9] I. El Hajj, L. Speyer, S. Cahen, L. Herbuvaux, P. Lagrange, G. Medjahdi, C. Hérold, Intercalation of barium into graphite by molten salts method: Synthesis of massive samples for crystal structure determination of BaC_6, Carbon. 186 (2022) 431-436. https://doi.org/10.1016/j.carbon.2021.09.073

[10] I. El Hajj, L. Speyer, S. Cahen, P. Berger, G. Medjahdi, P. Lagrange, C. Hérold, Co-intercalation into graphite of lithium, potassium and barium using LiCl-KCl molten salt, Carbon Lett. (2022). https://doi.org/10.1007/s42823-022-00352-8

[11] I. El Hajj, Le mélange eutectique LiCl-KCl fondu : un nouveau milieu pour l'intercalation dans le graphite d'alcalino-terreux et de lanthanoïdes, PhD thesis, Université de Lorraine (2022).

[12] S. Y. Leung, M. S. Dresselhaus, C. Underhill, T. Krapchev, G. Dresselhaus, J. Wuensch, Structural studies of graphite intercalation compounds using (00*l*) X-ray diffraction, Phys. Rev. B. 24 (1981) 3505-518. https://doi.org/10.1103/PhysRevB.24.3505

[13] P. Lagrange, M. Fauchard, S. Cahen, C. Hérold, Exhaustive inventory of 2D unit cells commensurate with honeycomb graphene structure, Carbon. 94 (2015) 919–927. https://doi.org/10.1016/j.carbon.2015.07.060

[14] M. Mayer, 15th International Conference on the Application of Accelerators in Research and Industry 475 (1999) 541–544.

[15] S. Bashkin, H. T. Richards, Proton bombardment of the lithium isotopes, Phys. Rev. 84 (1951) 1124–1129. https://doi.org/10.1103/PhysRev.84.1124

[16] R. Amirikas, D. N. Jamieson, S. P. Dooley, Measurement of (p, p) elastic cross sections for C, O and Si in the energy range 1.0-3.5 MeV, Nucl. Instrum. Methods in Physics Res. B. 77 (1993) 110-116. https://doi.org/10.1016/0168-583X(93)95531-9

[17] A. F. Gurbich, Evaluation of non-Rutherford proton elastic scattering cross section for oxygen, Nucl. Instrum. Methods in Physics Res. B. 129 (1997) 311–316. https://doi.org/10.1016/S0168-583X(97)00288-7

[18] I. Bogdanović, S. Fazinić, M. Jakšić, T. Tadić, O. Valković, V. Valković, Proton elastic scattering from fluorine, chlorine, zinc, selenium and bromine in the energy region from 2.5 to 4.8 MeV, Nucl. Instrum. Methods in Physics Res. B. 79 (1993) 524–526. https://doi.org/10.1016/0168-583X(93)95405-T

[19] R. J. De Meijer, A. A. Sieders, H. A. A. Landman, G. De Roos, Investigation of proton induced resonance reactions on 39 K, Nucl. Phys. A. 155 (1970) 109–128. https://doi.org/10.1016/0375-9474(70)90081-3

[20] S. Pruvost, P. Berger, C. Hérold, P. Lagrange, Nuclear microanalysis: an efficient tool to study intercalation compounds containing lithium, Carbon. 42 (2004) 2049-2056. https://doi.org/10.1016/j.carbon.2004.04.018

[21] P. Lagrange, A. Bendriss-Rerhrhaye, Etude de l'insertion dans le graphite des alliages binaires K-Bi, Rb-Bi et Cs-Bi, Carbon. 26 (1988) 283–289. https://doi.org/10.1016/0008-6223(88)90217-5

[22] A. Essaddek, P. Lagrange, F. Rousseaux, Structure of the intercalated metallic sheets in the lamellar graphite-cesium-antimony phases, Synth. Met. 34 (1989) 255–260. https://doi.org/10.1016/0379-6779(89)90394-9